



**University of Brasília - UnB  
Faculty UnB Gama - FGA  
Major of Aerospace Engineering**

**DESIGN AND NUMERICAL ANALYSIS OF GAS  
TURBINE BLADE PROFILES**

**Author: Hugo Felipe da Silva Lui  
Advisor: Prof. Domenico Simone, PhD**

**Brasília, DF  
2016**



**HUGO FELIPPE DA SILVA LUI**

**TITLE: DESIGN AND NUMERICAL ANALYSIS OF GAS TURBINE BLADE  
PROFILES**

A dissertation submitted in partial fulfilment  
of the requirements for the title of bachelor  
in Aerospace Engineering at the University  
of Brasília (FGA).

Adivisor: Prof. Domenico Simone, PhD

**Brasília, DF  
2016**

## CIP – Catalogação Internacional da Publicação\*

da Silva Lui, Hugo Felipe.

Title of dissertation: Design and numerical analysis of gas turbine blade profiles / Hugo Felipe da Silva Lui.

Brasília: UnB, 2016. 62 p. : il. ; 29,5 cm.

Dissertation (Undergraduate) – University of Brasília  
Faculty of Gama, Brasília, 2016. Advisor: Prof. Domenico  
Simone, PhD.

1. Axial turbine. 2. Computational fluid dynamics. 3. Gas turbine profile I. Simone, Domenico. II. PhD.

CDU Classificação

# DESIGN AND NUMERICAL ANALYSIS OF GAS TURBINE PROFILES

**Hugo Felipe da Silva Lui**

A dissertation submitted in partial fulfilment of the requirements for the title of bachelor in Aerospace Engineering at the University of Brasília (FGA) at 27/06/2016, defended, and approved by Dissertation Committee:

---

**Prof. PhD: Domenico Simone, UnB/ FGA**  
Advisor

---

**Prof. PhD: Paolo Gessini, UnB/ FGA**  
Committee Member

---

**Prof. PhD: Olexiy Shynkarenko, UnB/FGA**  
Committee Member

Brasília, DF  
2016

Esse trabalho é dedicado à minha mãe, Isamar da Silva, à minha família e a todos os meus amigos, que me apoiaram durante a minha vida.

## **AGRADECIMENTOS**

Eu agradeço a minha mãe por ter me apoiado durante minha graduação, sem o seu apoio, eu não chegaria a esse ponto. Eu agradeço também aos meus familiares pelo suporte dado. Um agradecimento especial aos meus amigos, os que fiz no CECB, na UnB e nos Estados Unidos, que foram essências para o meu amadurecimento pessoal e acadêmico.

Destaco também o quão importante foram o Professor Paniagua e o pesquisador Jorge, ambos da Purdue University, para esse trabalho. Sou muito grato ao Prof. Paniagua por me ter dado a oportunidade de trabalhar com turbinas axiais e também pelos seus conselhos. Sou extremamente agradecido ao Jorge, por ter sido meu mentor durante o meu estágio de pesquisa, suas “aulas” sobre turbinas axiais foram de grande ajuda para o desenvolvimento desse trabalho.

Agradeço ao Professor Domenico pela sua paciência e tempo para discussão desse trabalho e principalmente pelas suas sugestões cirúrgicas. Um agradecimento especial a todos os professores, seus ensinamentos foram de suma importância para a concretização desse trabalho.

“They did not know it was impossible, so they did it” - Jean Cocteau

## RESUMO

A demanda por motores aeronáuticos cada vez mais eficientes faz com que os projetistas de turbinas axiais procurem desenvolver pás que permitem fornecer tal performance requerida. O projeto da pá, começa a partir da definição dos perfis da pá em diferentes seções, geralmente em três posições: na raiz, no meio e no topo da pá. A forma 3D da turbina axial é obtida a partir do empilhamento dos perfis, da raiz até o topo da pá. A performance aerodinâmica da pá é afetada significativamente pela geometria do perfil. Dessa maneira, a definição do aerofólio possui papel crítico durante o projeto. Esse trabalho apresenta uma metodologia para o desenvolvimento de aerofólios para turbinas axiais, através do projeto 1D da turbina axial, junto com um método para gerar aerofólios usando curvas de Bézier. Primeiramente, será estudado a cascata de aerofólios da turbina VKI LS-89, como caso teste, para aprimoramento das técnicas em modelagem CFD. Posteriormente, simulações computacionais serão realizadas para verificação da qualidade dos aerofólios gerados, que será avaliada por meio dos gráficos de distribuição de pressão e número de Mach ao longo das superfícies do perfil aerodinâmico, além dos campos do escoamento. As simulações numéricas serão feitas pelo software ANSYS Fluent.

**Palavras-chave:** Turbina axial. CFD. Aerofólio. Turbinas a gás. Fluent. Curva de Bézier. Turbomáquinas



## ABSTRACT

The demand for increasingly efficient aircraft engines make turbine designers attempt to develop blades that provide such required performance. The blade design starts from the definition of blade profiles in different positions, usually in three places: hub, mid and tip sections. The 3D shape of an axial turbine is obtained by stacking the defined profiles from hub to tip. The aerodynamic performance of the blade is significantly affected by the profile geometry. Thus, the determination of the airfoil shape has critical role during the project. This work presents a methodology for developing airfoils for axial turbines through an 1D turbine design, along with a method for generating airfoils using Bezier curves. The VKI LS-89 transonic turbine cascade will be first studied as a test case for improvement of CFD modelling techniques. After that, CFD simulations will be performed in order to check the quality of the airfoils generated by evaluating the pressure and Mach number distribution along the airfoil surfaces, and the flow field contours. These numerical simulations will be carry out using the software ANSYS Fluent.

**Keywords:** Axial turbine. CFD. Airfoil. Gas turbine. Fluent. Bézier curve. Turbomachinery

## CONTENTS

<b>1 INTRODUCTION</b> .....	<b>11</b>
1.1 STATE OF ART .....	11
1.2 OBJECTIVES.....	13
1.3 WORK ORGANIZATION .....	14
<b>2 BASIC PRINCIPLES</b> .....	<b>15</b>
2.1 FUNDAMENTAL LAWS AND EQUATIONS .....	15
2.2 THE CONTINUITY EQUATION .....	16
2.3 THE MOMENTUM EQUATION .....	16
2.4 THE ANGULAR MOMENTUM EQUATION .....	18
2.6 THE FIRST LAW OF THERMODYNAMICS .....	19
2.6 THE SECOND LAW OF THERMODYNAMICS.....	20
2.7 THE IDEAL GAS EQUATION .....	22
2.8 COMPRESSIBLE FLOW EQUATION .....	22
<b>3 AXIAL FLOW TURBINE</b> .....	<b>25</b>
3.1 TURBINE GEOMETRY.....	25
3.2 VELOCITY DIAGRAMS OF THE AXIAL TURBINE STAGE.....	27
3.3 TURBINE DESIGN PARAMETERS.....	30
3.4 THERMODYNAMICS OF THE AXIAL TURBINE STAGE .....	33
3.5 EFFICIENCY.....	34
3.6 TURBINE SOURCE LOSS .....	35
3.7 ZWEIFEL CRITERION.....	38
<b>4 ONE DIMENSIONAL DESIGN PROCEDURE</b> .....	<b>40</b>
4.1 METHODOLOGY.....	40
4.2 DESIGN MODEL .....	41
4.3 TURBINE DESIGN PROCEDURE .....	42
<b>5 TURBINE AIRFOIL DESIGN</b> .....	<b>55</b>
5.1 BLADE PROFILE METHODS.....	55
5.2 BÉZIER CURVES .....	55
5.3 DESIGN APPROACH .....	57
<b>REFERENCES</b> .....	<b>65</b>

# 1. INTRODUCTION

## 1.1 STATE OF ART

Axial flow turbines are machines that have been used in many fields, as aviation, oil and gas, power generation, Navy etc. The application of turbomachinery is a global one, thus any increase in axial turbine efficiency and performance could lead to a major economic impact worldwide [1]. General electric [2] reports that an improvement in efficiency by 1% leads to an estimate saving in aviation industry of £6.14 billion over 15 years for a country.

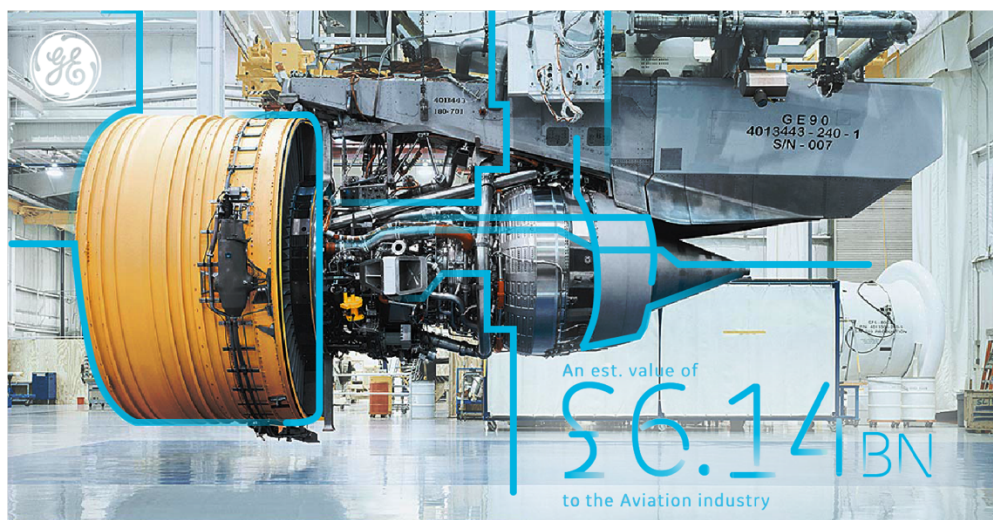


Figure 1. Estimate saving in aviation industry [2]

The fundamental components of aeronautical gas turbine engines, as illustrated in Fig. 2, are the compressor, the combustion chamber and the turbine. The compressor increases the static pressure of the air. In the combustion chamber, the fuel is mixed with this compressed air and burned, then the chemical energy stored by the fuel is converted in internal energy and pressure. The turbine extracts the energy from the working fluid leaving the combustion chamber. The power extracted by the turbine is used to drive the compressor. Finally, the energy available in the exhaust gases from the turbine is converted into a high speed propelling jet by the nozzle [3].

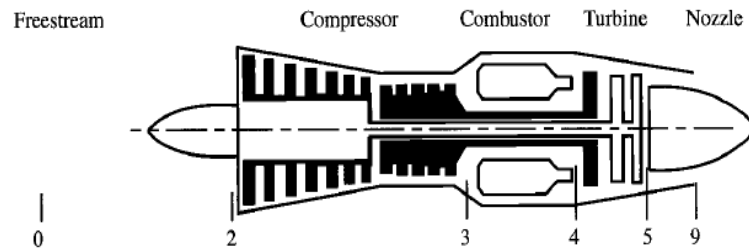


Figure 2. Typical single-spool turbojet [3]

For gas turbines engines, where axial turbines are employed, their net power output is the difference between the turbine work and compressor work, the ratio is about 2:1, so a small increase in efficiency of the compressor or turbine causes a larger proportional change in the power output, thus an increase in thrust for aeronautical gas turbine engines [1].

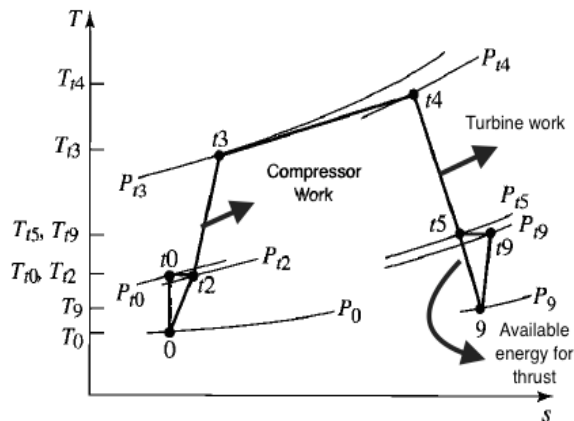


Figure 3. T-s diagram for a turbojet engine [3]

Over the years huge efforts have been expended in trying to improve the efficiency of axial turbines, and the total-to-total efficiency is now over 90 percent. This makes new improvements ever more difficult to achieve, however, it is still possible to obtain more efficient machines by improving the knowledge of the thermodynamics and fluid mechanics of the flow through the turbine [1].

The research on aircraft engines started in the 1940s and 1950s, it led to the development of several methods of performance of axial turbines, e.g., Ainley and Mathieson [6], which is still in use today. Over the years, new methods were developed by make some improvements on prediction of losses through the turbine, these different loss mechanisms are categorized as, profile loss, secondary or endwall loss and tip leakage. These improvements were possible due to the advent of new instrumentation, it led to a better understanding of the flow [1].

The advent of the high speed digital computer combined with the development of accurate numerical algorithms gave to engineers a new approach to study the flow, this new approach is called, computational fluid dynamics (CFD). It is basically a computer program which we can carry out “numerical experiments” to investigate the flow behavior and its properties [4].

CFD has been used as design tool by engineers to improve the turbine efficiency, decreasing the flow losses by blade geometry optimization. During the design the turbine blade designer make several adjusts on blade geometry in order to obtain the suitable geometry that combines good aerodynamic performance with structure requirements. This process of refinement of blade to match the better geometry can be time consuming and expensive. Therefore, optimization techniques such as evolutionary algorithms or inverse design methods are option to enhance the design process [5].

## **1.2 OBJECTIVES**

The main goal of this work is to develop a turbine airfoil design procedure based on existing methods. Thus, the blade profiles generated will be analyzed using 2D CFD simulations. A method to perform an axial turbine mean line design will be showed in order to provide the essential parameters to design the blade profiles. Also, one of the

aims of the work is to learn about CFD techniques, such as mathematical models used on CFD simulations, mesh generation, turbulence models and boundary layer.

### **1.3 WORK ORGANIZATION**

In the chapter 2, the basic principles of thermodynamic and fluid mechanics needed to analyze axial flow turbines will be demonstrated. In the chapter 3 discusses, the velocity triangles of a turbine stage, the design parameters, the thermodynamics of an axial turbine stage, 2D turbine losses, and efficiencies. In chapter 4, one dimensional turbine design procedure will be showed, in order to calculate the flow properties at each station of the turbine stage, the blade angles, and the blade row geometry. In the chapter 5, a turbine airfoil design procedure based on existing methods will be presented.

## **2 BASIC PRINCIPLES**

### **2.1 THE FUNDAMENTAL LAWS AND EQUATIONS**

According to Dixon and Hall [7], the basic physical laws of thermodynamics and fluid dynamics and equations necessary to the study of axial flow turbines are:

- i. The continuity equation
- ii. The momentum equation
- iii. The angular momentum equation
- iv. The first law of thermodynamics
- v. The second law of thermodynamics
- vi. The ideal gas Equation
- vii. Compressible flow relations

## 2.2 THE CONTINUITY EQUATION

From physical principle of mass conservation, “*Mass can be neither created nor destroyed*” [8]. The continuity equation is expressed by

$$\frac{\partial}{\partial t} \iiint_{cv} \rho dV + \iint_{cs} \rho \vec{V} \cdot d\vec{A} = 0 \quad (1)$$

The first integral term represents the time rate of change of the mass inside the control volumes, and the second integral term is the net mass flow into the control volume through the entire control surface

Most of axial flow turbine analyses are limited to steady and one-dimensional flows. Considering that we have an inlet and outlet surface, and assuming that there is no change within the control volume, then

$$\dot{m} = \rho_{in} V_{in} A_{n,in} = \rho_{out} V_{out} A_{n,out} \quad (2)$$

Where  $\rho$  is the fluid density,  $V$  is the velocity,  $A_n$  is the normal area.

## 2.3 THE MOMENTUM EQUATION

The momentum equation is based on Newton’s second law of motion. It expresses the sum of external forces acting on a fluid element to the rate of change of momentum in the direction of the resultant force. This equation is important because the force exerted upon a turbine blade can be obtained by found by the momentum equation [10]. The linear momentum equation is:



$$\iint_{CS} \vec{F} dA + \iiint_{CV} \vec{B} \rho dV = \frac{\partial}{\partial t} \iiint_{CV} \vec{V} (\rho dV) + \iint_{CS} \vec{V} (\rho \vec{V} \cdot d\vec{A}) \quad (3)$$

Here  $\vec{F}$  is the surface force (tangential and normal) per unit of area acting on the control surface,  $\vec{B}$  is the body force per unity mass, such as electromagnetic and gravity.

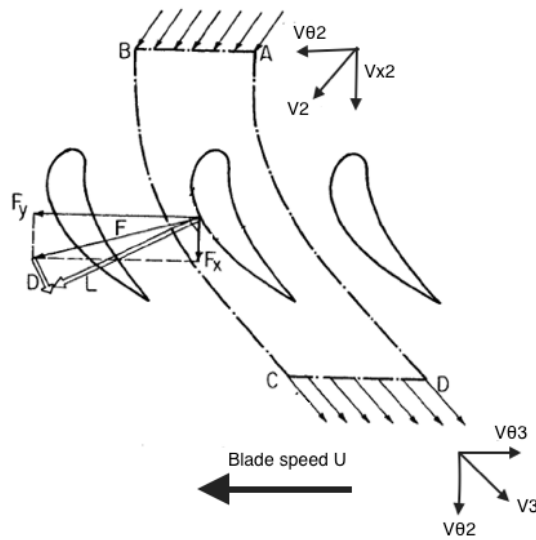


Figure 4. Control volume of a turbine cascade [10]

Considering a control volume of Fig. 4, for a steady state flow and assuming that inlet and outlet surfaces are far upstream and downstream, respectively, from the blade, where flow is uniform. The body forces acting on control volume is very small relative to the surface force, then  $\vec{B} \approx 0$ . Using the momentum equation, Eq. (3), applied to the control volume ABCD, the force in the tangential direction is given by:

$$F_y = \dot{m}(V_{\theta 2} - V_{\theta 3}) \quad (4)$$

Where  $V_{\theta 2}$  and  $V_{\theta 3}$  are the tangential velocities.

## 2.4 THE ANGULAR MOMENTUM EQUATION

The angular momentum relates the rate change of angular momentum of the system with the sum of moments of all external forces acting on the system [11]. It is based on one of the most important principles in mechanics, Newton's second law of motion. The angular momentum equation is given by

$$\sum M_0 = \frac{\partial}{\partial t} \iiint_{CV} (\vec{r} \times \vec{V}) \rho dV + \iint_{CS} (\vec{r} \times \vec{V}) \rho \vec{V} \cdot d\vec{A} \quad (5)$$

Where  $M_0$  is the moment about some point and  $r$  is the vector position.

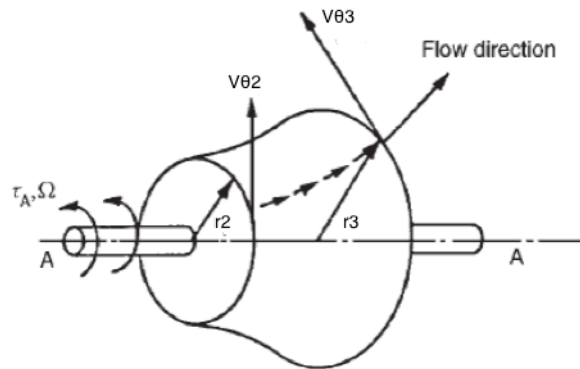


Figure 5. Control volume of a turbomachinery [7]

For a control volume as Fig. 5, where the fluid enters steadily at a uniform tangential velocity  $V_{\theta 2}$  and radius  $r_2$  and leaves with uniform velocity  $V_{\theta 3}$  and radius  $r_3$ , using Eq. (5), the torque about axis A is given by:

$$\tau_A = \dot{m}(r_2 V_{\theta 2} - r_3 V_{\theta 3}) \quad (6)$$

By Eq. (6), we can express the power generated by the turbine based on the tangential velocities

$$\dot{W} = \tau_A \Omega = \dot{m}(U_2 V_{\theta 2} - U_3 V_{\theta 3}) \quad (7)$$

Where  $\Omega$  is the angular velocity and the blade speed  $U = \Omega r$

## 2.5 THE FIRST LAW OF THERMODYNAMICS

The first law of thermodynamics states that *energy can be neither created nor destroyed during a process*, it can only change forms [9]. For an open system, the energy can be transfer by work  $W$ , heat  $Q$ , and by a flowing fluid. The energy of the system  $E$  is composed by: internal, kinetic, potential energy.

Considering a fluid which passes through a control volume at a steady rate mass flow  $\dot{m}$ , there is an inlet and outlet surface. Then, the first law of thermodynamics becomes

$$\begin{aligned} (\dot{Q}_{in} - \dot{Q}_{out}) + (\dot{W}_{in} - \dot{W}_{out}) + \dot{m}_1 \left( h_{in} + \frac{1}{2} V_{in}^2 + g z_{in} \right) \\ - \dot{m}_{out} \left( h_{out} + \frac{1}{2} V_{out}^2 + g z_{out} \right) = \frac{dE}{dt} \end{aligned} \quad (8)$$

Where  $\dot{W}$  is the rate of work transfer,  $\dot{Q}$  is the rate of heat transfer,  $U$  is the internal energy,  $g$  is the gravity and  $z$  is the height.

For convenience is useful to combine the enthalpy with the kinetic energy, the result is called the total enthalpy:

$$h_0 = h + \frac{1}{2} V^2 \quad (9)$$

The energy is transferred from the fluid to the turbine blades. Assuming that there is no heat transfer from or to the control volume surrounding, the variation of potential energy is negligible. As the turbine usually operates at steady state conditions, using Eq. (9) into Eq. (8), we have that the power generated by the turbine is

$$\dot{W} = \dot{m}(h_{\text{in}} - h_{\text{out}}) \quad (10)$$

Assuming that the working fluid is a thermally and calorically gas, which means that the specific heats ( $C_p$  and  $C_v$ ) are function of temperature only and they are constant. Thus,  $h = C_p T$ ,  $u = C_v T$  and the ratio of the specific heats is  $\gamma = \frac{C_p}{C_v}$ . In this way, we can express the enthalpy in terms of temperature. Thus, Eq. (10) becomes

$$\dot{W} = \dot{m}C_p(T_{\text{in}} - T_{\text{out}}) \quad (11)$$

Combining Eq. (7) with Eq. (10), results the Euler work equation

$$\Delta h_o = \Delta(UV_\theta) \quad (12)$$

This equation is valid for steady, adiabatic, viscous and inviscid flows and It states that greater the total enthalpy or tangential velocity change of the rotor, higher the power delivery by the turbine. Note that for stationary blades, the blade speed is zero, thus there is no work transfer from the fluid.

## 2.6 THE SECOND LAW OF THERMODYNAMICS

According to Cengel [9], the second law of thermodynamics asserts that processes occur in a certain direction and energy has quality. The process take place only if it satisfies the first and second law of thermodynamics. An important corollary of

the second law of thermodynamics, known as the inequality of Clausius. It introduces a new thermodynamic property, called entropy  $S$ . Considering state 1 as the start and state 2 as the end of the process, then

$$S_2 - S_1 = \int_1^2 \frac{\delta Q}{T} + S_{gen} \quad (13)$$

Where  $S_{gen}$  is the entropy generated during a process and it always positive quantity or zero. If the process is adiabatic,  $\delta Q = 0$ , then  $S_2 \geq S_1$ , if the process is reversible then,  $S_{gen} = 0$ . Thus, for a flow that is both adiabatic and reversible, the entropy will remain unchanged, this process as know as isentropic. Usually, axial turbine operates close to an isentropic process, therefore preliminary calculations are considered as adiabatic and reversible process, after that it is correct by some loss prediction method.

The first law of the thermodynamics can be expressed using the entropy definition and considering that the flow work (fluid pushed into or out of the control volume) is given by  $\delta w = P v$ . Assuming that the system is stationary and there is no potential energy. Using the entropy, internal energy and volume as specific properties then

$$T ds = du + p dv \quad (14)$$

or

$$T ds = dh + v dp \quad (15)$$

Equations (14) and (15) are called  $Tds$  equations and they are very useful, because the equations are written only in terms of properties of the system.

Based on definition of specific heats, we can express Eq. (14) and (15) in the following forms

$$s_2 - s_1 = C_p \ln \frac{T_2}{T_1} - \mathcal{R} \ln \frac{p_2}{p_1} \quad (16)$$

$$s_2 - s_1 = C_v \ln \frac{T_2}{T_1} + \mathcal{R} \ln \frac{v_2}{v_1} \quad (17)$$

Where  $\mathcal{R}$  is the gas constant.

## 2.7 THE IDEAL GAS EQUATION

The most important thermodynamic properties of the fluid are the pressure  $p$ , the temperature  $T$ , the density  $\rho$ , the enthalpy  $h$ , the entropy  $s$  and the specific heats  $C_p$  and  $C_v$ . We need to understand how these thermodynamic properties change during a flow process. Thus, there are equations that provides the relationship among those.

By Turns [2], the ideal gas equation relates the pressure  $p$ , the temperature  $T$  and the density  $\rho$  or the volume  $\mathcal{V}$  of an ideal gas, which are all gases at low pressures and at high temperatures, it is expressed as

$$p = \rho \mathcal{R} T \quad (18)$$

## 2.8 COMPRESSIBLE FLOW EQUATIONS

The Mach number is defined as the velocity divided by the local speed of sound  $a$ . For a perfect gas, the Mach number is written as

$$M = \frac{V}{a} = \frac{V}{\sqrt{\gamma \mathcal{R} T}} \quad (19)$$

Axial turbines operate in a range of Mach number that exceeds 0.3. According to Anderson [4] at this point the flow becomes compressible, therefore the fluid density can no longer be considered as constant.

Assuming a steady state flow, for an ideal gas undergoing isentropic process, no work ( $\dot{W} \approx 0$ ), the variation of potential energy is negligible ( $\Delta PE \approx 0$ ) and considering that the flow is brought to rest, then Eq. (8) can be expressed as

$$\frac{T_o}{T} = 1 + \frac{\gamma - 1}{2} M^2 \quad (20)$$

This equation represents the total temperature  $T_o$ , which is the static temperature measured when the flow is brought isentropically to rest.

Assuming an isentropic process ( $\Delta s = 0$ ) and manipulating Eq. (16) and Eq. (17), we obtain equations that relates the temperature, density and pressure

$$\frac{T_o}{T} = \left(\frac{\rho_o}{\rho}\right)^{\gamma-1} = \left(\frac{p_o}{p}\right)^{\frac{\gamma-1}{\gamma}} \quad (21)$$

Substituting Eq. (20) into Eq. (21), we can express the total density  $\rho_o$  and the total pressure  $p_o$  as function of Mach number and the ratio of specific heats

$$\frac{\rho_o}{\rho} = \left(1 + \frac{\gamma - 1}{2} M^2\right)^{\frac{1}{\gamma-1}} \quad (22)$$

$$\frac{p_o}{p} = \left(1 + \frac{\gamma - 1}{2} M^2\right)^{\frac{\gamma}{\gamma-1}} \quad (23)$$

For Dixon and Hall [7], one of the most important compressible flow equation for turbomachinery is the nondimensional mass flow rate, sometimes called as capacity equation. It is obtained by combining Eqs. (21), (22) and (23) with continuity, Eq. (2):

$$\frac{\dot{m}\sqrt{C_p T_o}}{A_n p_o} = \frac{\gamma}{\sqrt{\gamma-1}} M \left( 1 + \frac{\gamma-1}{2} M^2 \right)^{-\frac{1}{2} \left( \frac{\gamma+1}{\gamma-1} \right)} \quad (24)$$

From capacity equation, we can relate the flow properties, such as total temperature, total pressure, Mach number, and the thermodynamic properties of the gas with the nondimensional mass flow rate.

The compressible flow equations showed previously can be applied in the relative reference frame within the rotor blade rows. In this situation, the relative Mach number and stagnation properties are used:

$$\frac{T_{o,rel}}{T}, \frac{p_{o,rel}}{p}, \frac{\rho_{o,rel}}{\rho}, \frac{\dot{m}\sqrt{C_p T_{o,rel}}}{A_n p_{o,rel}} = f(M_{rel}) \quad (25)$$



### 3 AXIAL FLOW TURBINES

#### 3.1 TURBINE GEOMETRY

The turbine terminology used in this work is based on the schematic turbine configurations shown in Fig. 6 and Fig. 7 and summarized in Table. 1.

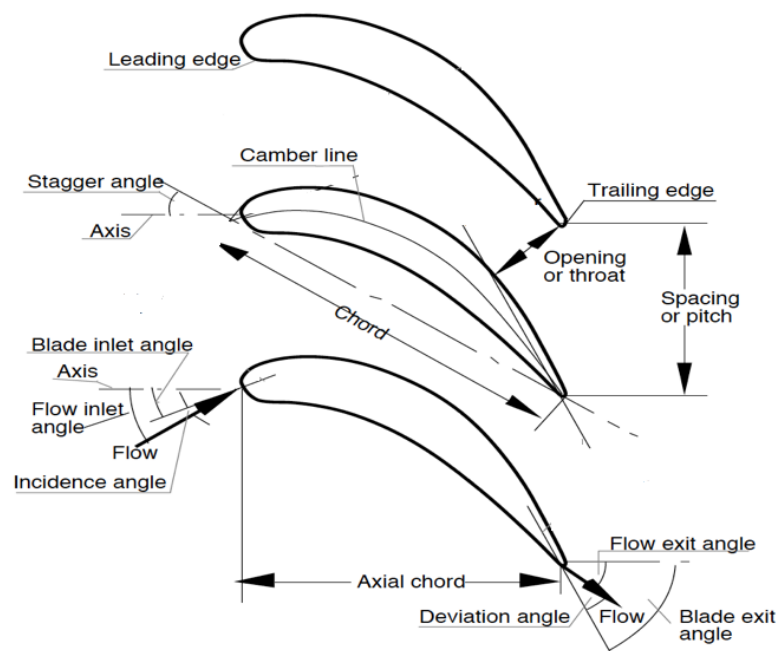


Figure 6. Turbine cascade geometry [15]

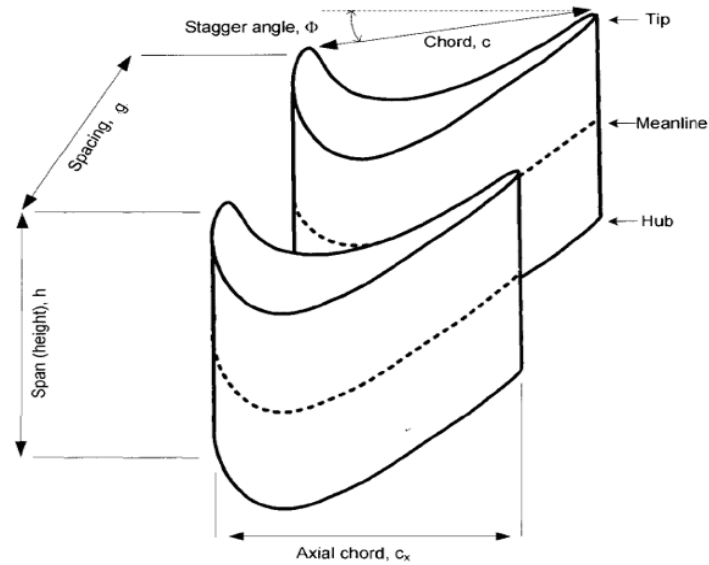


Figure 7. Blade geometry [16]

Table 1. Turbine geometry parameters

Name	Definition
Leading edge	It is the foremost edge of the turbine airfoil.
Trailing edge	It is the rearmost edge of the turbine airfoil.
Camber line	It is curve which the profile thickness distribution is symmetric.
Stagger angle, $\phi$	The angle between the chord line and the axial direction.
Spacing or pitch, $g$	The distance between corresponding points on adjacent blades.
Chord, $c$	The linear distance between the leading edge and the trailing edge.
Axial chord, $c_x$	It is axial length of the blade.
Incidence angle, $i$	The difference between the inlet flow angle $\alpha_1$ and the blade metal inlet angle $\alpha_1'$ . $i = \alpha_1 - \alpha_1'$

Deviation angle, $\delta$	The difference between the outlet flow angle $\alpha_2$ and the blade metal outlet angle $\alpha_2'$ . $\delta = \alpha_2 - \alpha_2'$
Pitch – chord ratio, $g/c$	The ratio of the pitch $g$ to the chord $c$ .
Aspect ratio, $h/c$	The ratio of the blade height $h$ to the chord $c$ .
Trailing edge blockage, $o/t_{te}$	The ratio of throat $o$ to the trailing edge thickness $t_{te}$ .

### 3.2 VELOCITY DIAGRAMS OF THE AXIAL TURBINE STAGE

The axial turbine stage comprises a row of stationary blades often called as stator or nozzle and a row of moving blades, known as rotor. The fluid enter the stator with absolute velocity  $V_1$  at angle  $\alpha_1$ , the pressure drop through the stator from pressure  $p_1$  to pressure  $p_2$  causes an acceleration from absolute velocity  $V_1$  to the absolute outlet velocity  $V_2$  at angle  $\alpha_2$ . The rotor inlet relative velocity  $w_2$  is calculated by subtracting, vectorially, the blade speed  $U$  from the absolute velocity  $V_2$  and define the relative inlet flow angle  $\beta_2$ . A further pressure drop from pressure  $p_2$  to pressure  $p_3$  through the rotor accelerates the flow from the inlet relative velocity  $w_2$  to the outlet relative velocity  $w_3$  and the flow leaves the rotor at a relative angle  $\beta_3$ . The corresponding absolute flow velocity  $V_3$  at angle  $\alpha_3$  is obtained by subtracting, vectorially, the outlet relative velocity  $w_3$  to the blade speed  $U$  [7].

The velocity triangles provide a better understanding of the relationship among absolute and relative flow velocities, and angles with the blade speed. The absolute velocities are aligned with stator inlet and outlet, and the relative velocities are aligned with the rotor inlet and outlet. All angles are measured from the axial ( $x$ ) direction and the sign convection is such that the tangential components of the velocities ( $V_\theta$  and  $w_\theta$ ) are positive if they point in the direction of the rotational speed and negative if they point into the opposite direction.

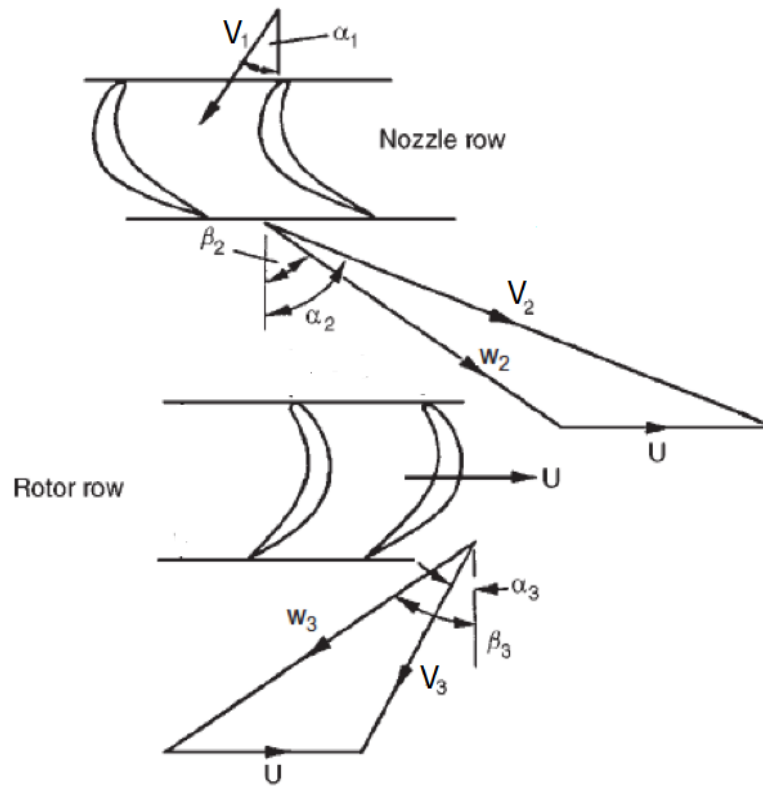


Figure 8. Turbine stage velocity triangles [7]

Based on Fig. 8, we can write the relations for absolute and relative flow angles for both stator and rotor:

$$V_{x2} = V_2 \cos \alpha_2 \quad (26)$$

$$V_{\theta 2} = V_2 \sin \alpha_2 \quad (27)$$

$$\tan \alpha_2 = \frac{V_{\theta 2}}{V_{x2}} \quad (28)$$

$$V_2 = \sqrt{V_{x2}^2 + V_{\theta 2}^2} \quad (29)$$

$$w_{x2} = w_2 \cos \beta_2 \quad (30)$$

$$w_{\theta 2} = w_2 \sin \beta_2 \quad (31)$$

$$\tan \beta_2 = \frac{w_{\theta 2}}{w_{x2}} \quad (32)$$

$$w_2 = \sqrt{w_{x2}^2 + w_{\theta 2}^2} \quad (33)$$

The relative velocity  $w$  is the vector subtraction of blade speed  $U$  from the absolute velocity  $V$ . From sign convection, the tangential component of velocities is positive, then

$$w_{\theta 2} = V_{\theta 2} - U \quad (34)$$

As the axial velocity is the same for both reference frames ( $V_{x2} = w_{x2}$ ), the relationship between the absolute and relative flow angles is given by:

$$\tan \beta_2 = \tan \alpha_2 - \frac{U}{V_{x2}} \quad (35)$$

For the rotor, we have

$$V_{x3} = V_3 \cos \alpha_3 \quad (36)$$

$$V_{\theta 3} = V_3 \sin \alpha_3 \quad (37)$$

$$\tan \alpha_3 = \frac{V_{\theta 3}}{V_{x3}} \quad (38)$$

$$V_3 = \sqrt{V_{x3}^2 + V_{\theta 3}^2} \quad (39)$$

$$w_{x3} = w_3 \cos \beta_3 \quad (40)$$

$$w_{\theta 3} = w_3 \sin \beta_3 \quad (41)$$

$$\tan \beta_3 = \frac{w_{\theta 3}}{w_{x3}} \quad (42)$$

$$w_3 = \sqrt{w_{x3}^2 + w_{\theta 3}^2} \quad (43)$$

From sign convection, for the rotor, the tangential component of velocities is negative, then

$$w_{\theta 3} = V_{\theta 3} + U \quad (44)$$

Being axial velocity the same for both reference frames ( $V_{x3} = w_{x3}$ ), thus

$$\tan \beta_3 = \tan \alpha_3 + \frac{U}{V_{x3}} \quad (45)$$

### 3.3 TURBINE DESIGN PARAMETERS

Three fundamentals nondimensional parameters that are very useful to design axial turbines: Flow Coefficient  $\phi$ , Stage Loading Coefficient  $\psi$  and Pressure Reaction

Degree  $R$ . These parameters have influence on the shape of the velocity triangles, which is related to the efficiency and number of stages [7].

The flow coefficient  $\phi$  is the ratio of the axial flow velocity  $V$  to the blade speed  $U$ .

$$\phi = \frac{V_x}{U} \quad (46)$$

High values of  $\phi$  mean small relative flow angles and velocities close to the axial direction. Low value of  $\phi$  imply wide relative flow angles with velocities close to the tangential direction.

The Stage Loading can be derived from Euler work equation (12), and defined as the ratio between the change of the intensity of the tangential component of  $V$  and the blade speed  $U$ .

$$\psi = \frac{\Delta V_\theta}{U} \quad (47)$$

High stage loading implies large flow turning ( $\Delta\beta = \beta_2 - \beta_3$ ). From Euler work equation (12) we can see that high stage loadings lead to high specific work, then fewer stages; however high stage loadings have influence on blading efficiency (increase in losses).

The Pressure Reaction Degree  $R$  is the most important turbine parameter because has influences on the efficiency and number of stages. Usually, a preliminary design calculation starts from the choice of the pressure reaction degree, defined as:

$$R = \frac{p_2 - p_3}{p_1 - p_3} \quad (48)$$

In fact, the degree of reaction is a free design parameter and the choice of its values depends on project requirements as high efficiency and small size [14]. Historically, the turbine designers opted either for zero degree of reaction or for the 50% reaction turbines. The effect of pressure reaction degree on the turbine design is illustrated in Fig. 9, where the comparison among different degrees of reaction is made assuming that the velocity triangles at the exit of the rotor are the same, the only changes being in the stator exit conditions.

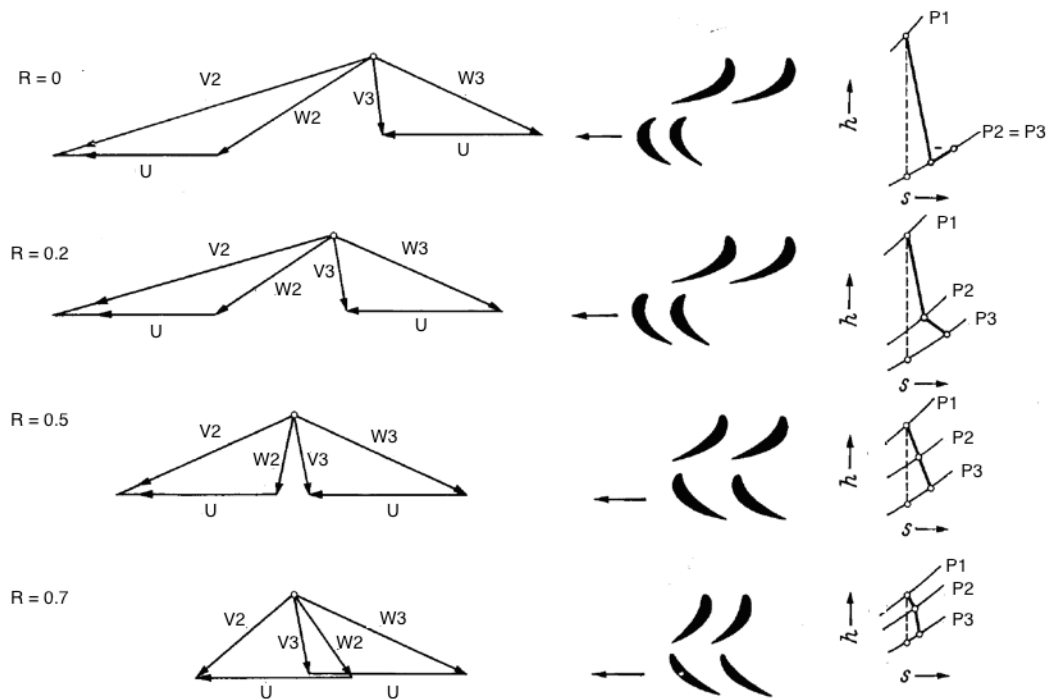


Figure 9. Effect of Pressure Reaction Degree on velocity triangles [14]

From Fig. 9, we can see that increasing the pressure degree of reaction  $R$ , the enthalpy drop  $\Delta h_o$  decreases; this is related to the decrease of the tangential component of the stator exit velocity  $V_{\theta 2}$ , explained by the Euler work equation (12). Being  $V_{\theta 3}$  constant, thus we have a reduction of work done by the turbine Eq. (7).

At zero pressure degree of reaction, the entire pressure drop happens in the stator, thus  $V_2$  and  $V_{\theta 2}$  have the maximum values, as well the absolute stator outlet flow angle  $\alpha_2$ . In the rotor, the relative flow angles ( $\beta_2$  and  $\beta_3$ ) and velocities ( $w_2$  and  $w_3$ ) are equal. The flow turning is maximum, then from Eq. (7), the work extracted by



the turbine is maximum compared with other pressure degree of reaction values. Often, this type of turbine is called impulse turbine.

At  $R = 0.5$ , the velocity triangles are equal, then:  $V_2 = w_2$ ,  $V_3 = w_2$ ,  $\alpha_2 = \beta_3$  and  $\beta_2 = \alpha_3$ , these lead to a low flow turning and being the blading efficiency related to the turning, typically turbines designed with  $R = 0.5$  have the highest efficiency but are delivering less work with respect, for example, to the case  $R = 0$ . For this reason, they are realized including more stages.

### 3.4 THERMODYNAMICS OF THE AXIAL TURBINE STAGE

The working process of the axial turbine is illustrated in the h-s diagram of Fig. 10. The thermodynamic process in the turbine stage depends on the pressure reaction degree; in order to explain it, a turbine with ( $R \approx 0.5$ ) has been chosen. The process through the stator or nozzle occurs along the curve 1-2, where the static pressure decreases from  $p_1$  to  $p_2$ . The change in total pressure ( $p_{02} - p_{01}$ ) is due to increase in entropy connected to viscous losses [6].

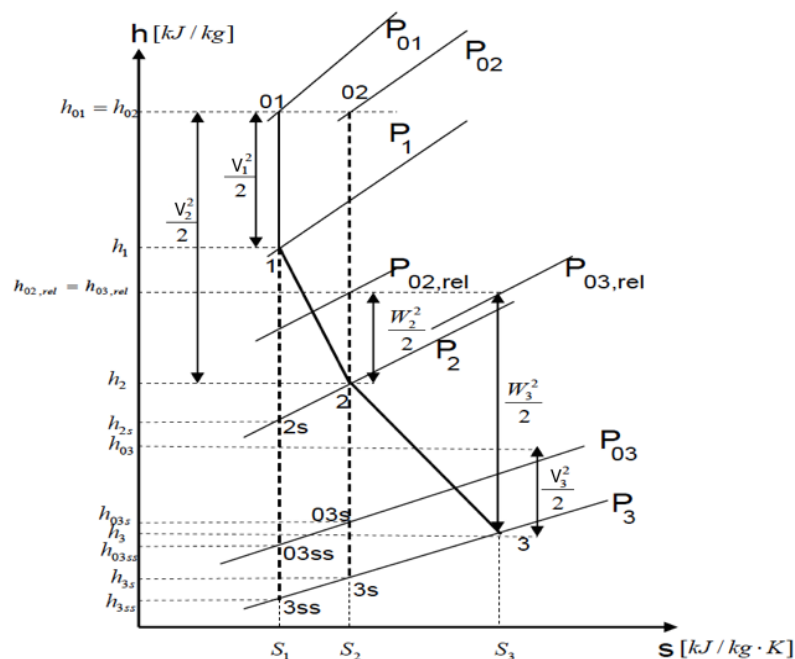


Figure 10. Expansion process in a turbine stage [17]

As there is no work extraction in the stator, the total enthalpy across the stator remains constant. From Eq. (10)

$$h_{01} = h_{02} \quad (49)$$

The working process in the rotor is represented by curve 2-3. In the rotor row, there is another pressure drop. The total enthalpy in the absolute frame is changing due to the energy transfer from the working fluid to the blades. In the rotor relative frame, we can't see the work extraction and thus we can consider constant the relative total enthalpy; so, from Eq. (10)

$$h_{02,rel} = h_{03,rel} \quad (50)$$

These two equations will be useful when the one-dimensional turbine design will be discussed.

### 3.5 EFFICIENCY

The turbine overall efficiency can be defined as the available energy in a flowing fluid converted into useful work delivered at the output shaft [7]. The isentropic efficiency  $\eta_t$  is a measure of the quality of this energy conversion. It is expressed by

$$\eta_t = \frac{\text{actual work}}{\text{ideal work}} = \frac{\Delta W}{\Delta W_{max}} \quad (51)$$

The ideal work depends on how the ideal process is defined. The maximum work will always be an isentropic process, but we need to designate the correct exit state of the ideal process relative to the actual process. It depends on whether the exit kinetic energy is usefully employed or wasted.

If the exhausting kinetic energy is usefully employed (as in the case of the last stage of aircraft gas turbines, where it contributes to the jet thrust or in the case of a multistage turbine, where kinetic energy exhausting from stage is used in the following stage), the ideal process is to the same total pressure as the actual expansion, then from Eq. (10), we can define the total-to-total efficiency  $\eta_{tt}$

$$\eta_{tt} = \frac{\Delta W}{\Delta W_{max}} = \frac{h_{01} - h_{03}}{h_{01} - h_{03s}} \quad (52)$$

If the exhausting kinetic energy cannot be usefully employed, (like when it is wasted directly to the surrounding), the ideal expansion is to the same static pressure as the actual expansion, then we can define the total-to-static efficiency  $\eta_{ts}$ ,

$$\eta_{ts} = \frac{\Delta W}{\Delta W_{max}} = \frac{h_{01} - h_{03}}{h_{01} - h_{3s}} \quad (53)$$

### 3.6 TURBINE LOSSES

According to Dixon and Hall [7] and Denton [1], the losses in a turbine can be divided in two types: 2D or 3D. 2D loss sources are due to blade boundary layer, trailing edge mixing and shock system. 3D sources are connected to tip leakage flows, endwall or secondary flows and coolant flows. In this work, only a 2D turbine will be investigated, then 3D losses are not considered.

The loss in the blade boundary layer is the work expended by the particles against the viscous forces; it depends on the development of the boundary layer, which is related to the blade surface pressure distribution, and in particular, to the transition from laminar to turbulent flow. Boundary layer loss typically is responsible for over 50% of the 2D loss in a subsonic turbine.

From Denton [1], the entropy loss coefficient for the blade boundary layers is given by:

$$\xi_b = 2 \sum \frac{L_b}{s \cos \alpha_2} \int_0^1 C_{dis} \left( \frac{V_b}{v_2} \right)^3 d \left( \frac{x}{L_b} \right) \quad (54)$$

Where,  $C_{dis}$  is the dissipation coefficient,  $V_b$  is the blade surface velocity and  $L_b$  is the blade surface length.

From Eq. (54), the term  $\left( \frac{V_b}{v_2} \right)^3$  shows that the suction side is dominant in loss production, as the suction side has regions of high surface velocities.

Another parameter that has a big role, is the dissipation coefficient  $C_{dis}$ . From Fig. 11, where either a laminar or a turbulent flow could exist ( $300 < Re_\theta < 1000$ ), the laminar dissipation coefficient  $C_{dis}$  is lower than the turbulent dissipation coefficient  $C_{dis}$ .

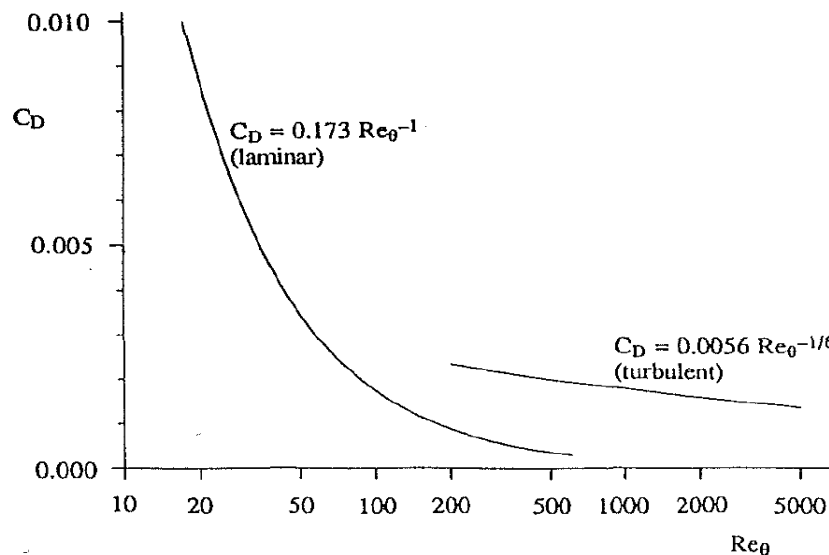


Figure 11.  $C_{dis}$  vs. Reynolds number based on momentum thickness  $Re_\theta$  [1]

Then, in order to minimize the loss, the boundary layer should be kept laminar for as long as possible. It depends on the Reynolds number, turbulence level, and the

blade surface velocity distribution. Therefore, the prediction of the boundary layer transition is very important in the turbine design.

One of the main sources of loss for turbines is the trailing edge mixing loss. The trailing edge mixing loss accounts for about 35% of the total 2D loss in subsonic turbines, and about 50% of the total 2D loss in supersonic turbines. The trailing edge mixing loss is related to the mixing of the suction surface and pressure surface boundary layers, which have different flow conditions, with the region of flow downstream the trailing edge

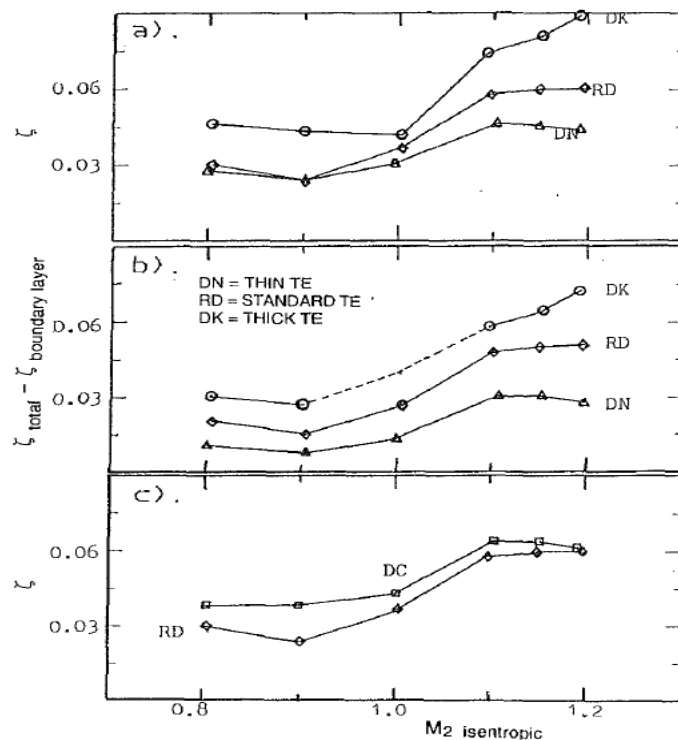


Figure 12. The variation of The trailing edge mixing loss with Mach number and trailing edge thickness [18]

Xu and Denton [18] states that the trailing edge loss increases roughly linearly with the trailing edge blockage (Table 1). Fig. 12 shows the results of a family of turbines with different trailing edge thicknesses. As we can see that when Mach number is higher than one, there is a large increase in the trailing edge loss; this happens because of the trailing edge shock system, mixing, and complex trailing edge flow pattern. Therefore, thick trailing edges are the best alternative to decrease the loss.

### 3.7 ZWEIFEL CRITERION

There is an optimum pitch to chord ratio that provides a minimum overall loss. The pitch to chord ratio has great influence on blade velocity distribution. Assuming that the blade chord is constant, if we increase the space between the blades, the friction losses are small, but we have a poor fluid guidance, which leads to high losses due to flow separation. If the pitch is low, the blades give the maximum amount of guidance to the fluid; however, the friction losses will be large. Zweifel [19] found that the ratio of an actual to an ideal tangential blade loading has an approximately constant value for minimum losses for blades having a high outlet angles. Based on Zweifel coefficient  $Z$ , the optimum pitch to chord ratio can be obtained.

The actual tangential blade load for the stator and rotor are given by Eq. (4):

$$-F_{y,s} = \dot{m}(V_{\theta 2} - V_{\theta 1}) \quad (55)$$

$$F_{y,R} = \dot{m}(w_{\theta 2} - w_{\theta 3}) \quad (56)$$

The condition of ideal load is when the inlet total pressure acts over the whole pressure surface and the outlet static pressure acts over the whole suction surface. Assuming that the blade height is constant. Then, the ideal tangential blade load for the stator and rotor is the difference of pressure between sides:

$$-F_{y\_ideal,s} = (p_{01} - p_2)hc \quad (57)$$

$$F_{y\_ideal,R} = (p_{02,rel} - p_3)hc \quad (58)$$

Being the Zweifel coefficient is the ratio of actual to an ideal tangential blade load

$$Z_s = \frac{\dot{m}(V_{\theta 2} - V_{\theta 1})}{(p_{01} - p_2)hc} \quad (59)$$

$$Z_R = \frac{\dot{m}(w_{\theta 2} - w_{\theta 3})}{(p_{02,rel} - p_3)hc} \quad (60)$$

Substituting Eq. (2) and into Eq. (59) and Eq. (60), we have

$$\left(\frac{g}{c}\right)_s = \frac{(p_{01} - P_2)Z}{\rho_2 V_{x2}(V_{\theta 2} - V_{\theta 1})} \quad (61)$$

$$\left(\frac{g}{c}\right)_R = \frac{(p_{02,rel} - P_3)Z}{\rho_2 V_{x2}(w_{\theta 2} - w_{\theta 3})} \quad (62)$$

Based on experiments on low Mach number turbine cascades, Zweifel [19] determined that the value of  $Z$  was approximately 0.8. According to Dixon and Hall [7], the Zweifel coefficient accurately predicts optimum pitch to chord ratio for outlet angles of  $60^\circ$  to  $70^\circ$ . The Zweifel coefficient may be greater than 1 in some cases, as low pressure turbines.

## 4 ONE DIMENSIONAL TURBINE DESIGN PROCEDURE

### 4.1 METHODOLOGY

The complete design of the turbine blade can be divided in 6 main activities as shown in Fig. 13 [20]. This thesis focus on the three first processes:

- 1) 1D turbine design
- 2) 2D Blade profile design
- 3) 2D CFD analysis

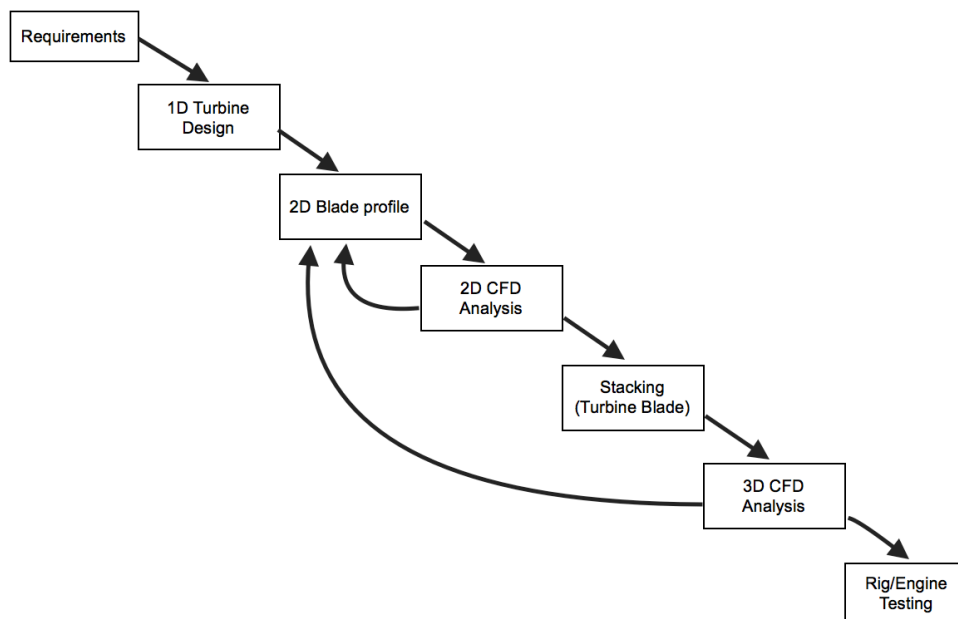


Figure 13. Flowchart of the Turbine blade design



The 1D turbine design is a critical part of the process, being the 80% of the final product defined in the 20% of the design time [20]. The primary optimization of the turbine geometry in terms of flow angles has been made by writing a first MATLAB code, the Meanline Analysis Program, described by the flowchart shown in Fig. 14, and presented in details in the following paragraphs. This program provides inlet and outlet flow angles, pitch, chord, that are the parameters required to design the 2D blade profiles. The stagger angle is obtained by using statistical data [21], as will be shown in the following paragraphs.

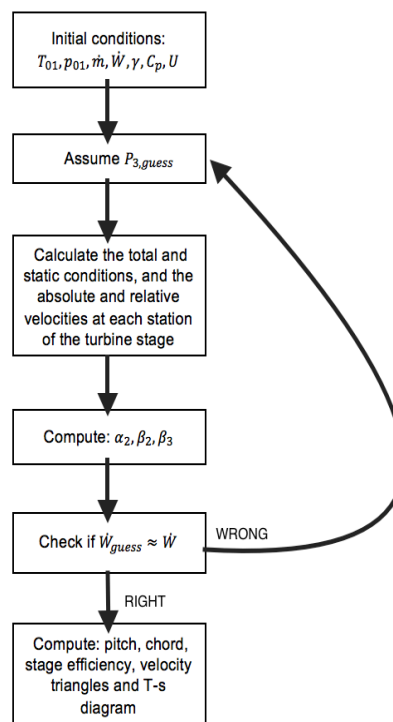


Figure 14. Flowchart of the Meanline Analysis Program

Finally, these parameters have been used to design the blade profile, following the Bézier curve method, implemented by writing another MATLAB code.

## 4.2 DESIGN MODEL

The one dimensional turbine design procedure used in this work has been developed by Sieverding [10]. The design starts with determination of pressure degree

of reaction. After that, the calculation of flow properties at the stator inlet and outlet (that are also the rotor inlet conditions), and rotor outlet is performed. The annulus areas are calculated, followed by the blade heights at each station. The blade row and channel geometries are thus determined. The flow properties are calculated at the mid span of the blade (meanline design).

The design procedure is an iterative method: being the static pressure at the exit of the turbine unknown, a first tentative value of the pressure is necessary; besides the blading efficiency depends on the inlet and outlet flow angles, Mach number, Reynolds number, pitch to chord ratio and aspect ratio and we don't know these values, the first calculations are performed assuming values of blading efficiencies based on statistical data [10]. In case of blading efficiencies, calculated by using loss models, different from the estimated values, the design calculation is repeated.

### 4.3 TURBINE DESIGN PROCEDURE

The initial data required to start the calculation are the total inlet temperature  $T_{01}$ , the total inlet pressure  $p_{01}$ , the mass flow rate  $\dot{m}$ , the power delivered by the turbine  $\dot{W}$ , the blade speed  $U$ , the specific heat ratio  $\gamma$ , and the specific heat at constant pressure  $c_p$ . The process is assumed to be adiabatic and will be assumed that the specific heat ratio  $\gamma$  and the specific heat at constant pressure  $C_p$  are constant through the turbine stage. The following equations have been implemented in a MATLAB code (Meanline Analysis Program) written by the author.

From the Pressure Degree of Reaction  $R$  chosen, we can calculate the stator outlet static pressure  $p_2$  by assuming a value of the rotor outlet static pressure  $p_3$  and considering  $p_1 \approx p_{01}$  (being the inlet Mach number low  $M_1 \approx 0.15 - 0.3$ ). From Eq. (48), we have

$$p_2 = R(p_{01} - p_1) + p_3 \quad (63)$$

Being the total enthalpy constant across the stator, Eq. (49), its inlet total temperature  $T_{01}$  is equal to the stator outlet total temperature  $T_{02}$ ; then from the isentropic relation between the temperature and pressure, Eq. (21), we can determine the isentropic static exit temperature  $T_{2,s}$

$$T_{2,s} = T_{01} \left( \frac{p_2}{p_{01}} \right)^{\frac{\gamma-1}{\gamma}} \quad (64)$$

From Eq. (9), we can find the stator isentropic absolute outlet velocity  $V_{2,s}$

$$V_{2,s} = \sqrt{2c_p(T_{01} - T_{2,s})} \quad (65)$$

Assuming a value of  $\eta_s = 0.92 - 0.93$  for the stator blading efficiency  $\eta_{ts,S}$  [10], we can calculate the static temperature  $T_2$ , from the definition of total-to-static efficiency, Eq. (53)

$$T_2 = T_{01} - \eta_{ts,S}(T_{01} - T_{2,s}) \quad (66)$$

The stator blading efficiency  $\eta_s$  can also be expressed as the ratio of the stator absolute outlet velocity  $V_2$  to the the isentropic stator outlet velocity  $V_{2,s}$ , then we can write:

$$V_2 = \sqrt{\eta_{ts,S}} V_{2,s} \quad (67)$$

The stator outlet density is calculated from the ideal gas equation, Eq. (18):

$$\rho_2 = \frac{p_2}{RT_2} \quad (68)$$

The stator outlet Mach number is determined from Eq. (19):

$$M_2 = \frac{V_2}{\sqrt{\gamma \mathcal{R} T_2}} \quad (69)$$

From isentropic relation, Eq. (21), the stator outlet total pressure  $p_{02}$  is calculated

$$P_{02} = P_2 \left( \frac{T_{01}}{T_2} \right)^{\frac{\gamma}{\gamma-1}} \quad (70)$$

Being the stator exit velocity  $V_2$  known, the stator absolute outlet axial velocity  $V_{x2}$  or the stator absolute outlet angle  $\alpha_2$  can be free choices of the designer. According to Sieverding [10], 90% of the high pressure turbines have the stator absolute outlet angle ranging from  $70^\circ$  to  $75^\circ$ . Moreover, most of low pressure turbines have the stator absolute outlet angle ranging  $60^\circ$  to  $70^\circ$ . Therefore, it is easy to choice the stator absolute outlet flow angle  $\alpha_2$ , and to obtain the components of the absolute velocity from Eq. (26) and (27),

$$V_{x2} = V_2 \cos \alpha_2 \quad (71)$$

$$V_{\theta 2} = V_2 \sin \alpha_2 \quad (72)$$

From Eq. (34), we can calculate the stator relative outlet tangential velocity  $w_{\theta 2}$

$$w_{\theta 2} = V_{\theta 2} - U \quad (73)$$

Being the axial velocity constant on both reference frames ( $V_{x2} = w_{x2}$ ), from Eq. (32), the stator outlet relative angle  $\beta_2$  is determined as

$$\tan \beta_2 = \frac{w_{\theta 2}}{w_{x 2}} \quad (74)$$

From Eq. (33), we have the stator outlet relative velocity  $w_2$

$$w_2 = \sqrt{w_{x 2}^2 + w_{\theta 2}^2} \quad (75)$$

The stator outlet total temperature and pressure at the relative reference frame are calculated from Eq. (9) and Eq. (21) respectively

$$T_{02,rel} = T_2 + \frac{w_2^2}{2C_p} \quad (76)$$

$$P_{02,rel} = P_2 \left( \frac{T_{02,rel}}{T_2} \right)^{\frac{\gamma}{\gamma-1}} \quad (77)$$

The stator relative outlet Mach number is determined from Eq. (19):

$$M_{2,rel} = \frac{w_2}{\sqrt{\gamma R T_2}} \quad (78)$$

The flow is accelerated in the rotor by an expansion process from the total inlet properties  $T_{02,rel}$  and  $P_{02,rel}$  to the the rotor outlet static pressure  $p_3$ . In the relative frame, the total enthalpy in the rotor is constant ( $T_{02,rel} = T_{03,rel}$ , Eq. (50)), thus from Eq. (21) we can calculate the isentropic static exit temperature  $T_{3,s}$

$$T_{3,s} = T_{03,rel} \left( \frac{p_3}{p_{02,rel}} \right)^{\frac{\gamma-1}{\gamma}} \quad (79)$$

From Eq. (9), we can find the rotor isentropic relative outlet velocity  $w_{3,s}$

$$w_{3,s} = \sqrt{2c_p(T_{03,rel} - T_{3,s})} \quad (80)$$

Being the value of the rotor blading efficiency  $\eta_{ts,R}$  ranging from 0.87 to 0.88 [10], we can calculate the static temperature  $T_3$ , from the definition of total-to-static efficiency, Eq. (53)

$$T_3 = T_{03,rel} - \eta_{ts,R}(T_{03,rel} - T_{3,s}) \quad (81)$$

Moreover, the rotor blading efficiency  $\eta_{ts,R}$  can be expressed as the ratio of the stator relative outlet velocity  $w_3$  to the the isentropic rotor relative outlet velocity  $w_{3,s}$ , thus we write  $w_3$  as

$$w_3 = \sqrt{\eta_{ts,R}} w_{3,s} \quad (82)$$

The rotor outlet density is calculated from the ideal gas equation, Eq. (18):

$$\rho_3 = \frac{p_3}{RT_3} \quad (83)$$

The rotor relative outlet Mach number is determined from Eq. (19):

$$M_{3,rel} = \frac{w_3}{\sqrt{\gamma RT_3}} \quad (84)$$

From isentropic relation, Eq. (21), the rotor relative outlet total pressure is calculated

$$P_{03,rel} = P_3 \left( \frac{T_{03,rel}}{T_3} \right)^{\frac{\gamma}{\gamma-1}} \quad (85)$$

To calculate the rotor conditions, we will assume that there is no change of the radius of the midspan line between the rotor inlet and rotor outlet. Then, the rotor absolute outlet axial velocity  $V_{x3}$  or the rotor relative outlet angle  $\beta_3$  can be free choices of the designer. Typically, it is considered that the absolute axial velocity remains constant through the rotor and being that the axial velocity the same for both reference frames, we have

$$V_{x3} = V_{x2} \quad (86)$$

$$w_{x3} = V_{x3} \quad (87)$$

From Eq. (42), we can obtain the rotor relative outlet angle  $\beta_3$

$$\beta_3 = \cos^{-1} \left( \frac{w_{x3}}{w_3} \right) \quad (88)$$

We can calculate the rotor relative outlet tangential velocity  $w_{\theta 3}$

$$w_{\theta 3} = w_3 \sin \beta_3 \quad (89)$$

The rotor absolute outlet tangential velocity  $V_{\theta 3}$  is given by Eq. (44)

$$V_{\theta 3} = w_{\theta 3} - U \quad (90)$$

From Eq. (38), the rotor absolute outlet angle  $\alpha_3$  is obtained

$$\alpha_3 = \tan^{-1} \frac{V_{\theta 3}}{V_{x3}} \quad (91)$$

We can calculate the rotor absolute velocity  $V_3$  by Eq. (39)

$$V_3 = \sqrt{V_{x3}^2 + V_{\theta 3}^2} \quad (92)$$

The rotor absolute outlet Mach number is determined from Eq. (19):

$$M_3 = \frac{V_3}{\sqrt{\gamma R T_3}} \quad (93)$$

The rotor outlet total temperature and pressure at the absolute reference frame are calculated from Eq. (9) and Eq. (21) respectively

$$T_{03} = T_3 + \frac{V_3^2}{2C_p} \quad (94)$$

$$P_{03} = P_3 \left( \frac{T_{03}}{T_3} \right)^{\frac{\gamma}{\gamma-1}} \quad (95)$$

Now, the power delivered by the turbine stage can be calculated from Eq. (7) or Eq. (11)

$$\dot{W}_i = \dot{m} C_p (T_{01} - T_{03}) \quad (96)$$



Or

$$\dot{W}_i = \dot{m}U(V_{\theta 2} - V_{\theta 3}) \quad (97)$$

If the power delivered by the stage  $\dot{W}_i$ , given by Eq. (96) or Eq. (97), is different from the power  $\dot{W}$  expected by the turbine designer, a new value of the rotor outlet static pressure  $p_3$  needs to be specified; then the design process, from Eq. (63) to Eq. (97), is repeated until the condition:

$$\frac{\|\dot{W} - \dot{W}_i\|}{\|\dot{W}\|} = 10^{-3} \quad (98)$$

The entropy increase  $\Delta s$  through the turbine stage is given by Eq. (16):

$$\Delta s_s = s_2 - s_1 = C_p \ln \frac{T_2}{T_1} - \mathcal{R} \ln \frac{p_2}{p_1} \quad (99)$$

$$\Delta s_R = s_3 - s_2 = C_p \ln \frac{T_3}{T_2} - \mathcal{R} \ln \frac{p_3}{p_2} \quad (100)$$

$$\Delta s = \Delta s_s + \Delta s_R \quad (101)$$

Where  $\Delta s_s$  and  $\Delta s_R$  are the entropy increases through the stator and rotor respectively.

If the exhaust velocity is usefully employed, the total-to-total efficiency is calculated from Eq. (52)

$$\eta_{ts} = \frac{\Delta W}{\Delta W_{max}} = \frac{h_{01} - h_{03}}{h_{01} - h_{03s}} \quad (102)$$

Otherwise, If the exhaust velocity cannot be usefully employed, the total-to-static efficiency is given by Eq. (53)

$$\eta_{ts} = \frac{\Delta W}{\Delta W_{max}} = \frac{h_{01} - h_{03}}{h_{01} - h_{3s}} \quad (103)$$

With the flow properties so defined, the calculation of flow areas can be performed, the annulus area of a turbine  $A_{annulus}$  being given by

$$A_{annulus} = \pi r_T^2 \left[ 1 - \left( \frac{r_H}{r_T} \right)^2 \right] \quad (104)$$

Using the continuity equation, Eq. (2), we can also calculate the annulus area of the stator outlet  $A_2$ :

$$A_2 = \frac{\dot{m}}{\rho_2 V_{x2}} \quad (105)$$

Notice that the ratio of hub radius  $r_H$  to tip radius  $r_T$  for high pressure turbines is typically  $\frac{r_H}{r_T} \approx 0.9$ , while, for low pressure turbines is ranging from 0.75 to 0.85 for front stage and from 0.60 to 0.65 for rear stage [10].

Combining Eq. (104), with Eq. (105), and using an appropriate value for  $\frac{r_H}{r_T}$ , we can calculate the tip radius  $r_{T2}$  for the stator outlet

$$r_{T2} = \sqrt{\frac{A_2}{\pi \left[ 1 - \left( \frac{r_H}{r_T} \right)^2 \right]}} \quad (106)$$

The stator blade height  $h_2$  is the difference between the tip radius and hub radius (Fig. 15).

$$h_2 = r_{T2} - r_{H2} \quad (107)$$

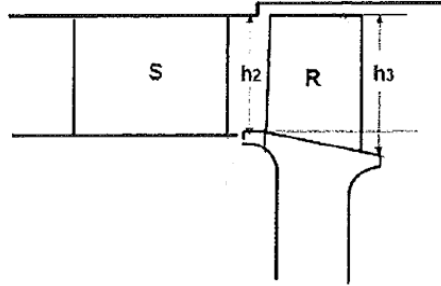


Figure 15. Meridional view of a turbine stage [10]

Typically, the hub radius remains constant through the stage, then  $R_{H3} = R_{H2}$ . The annulus area, the tip radius and the blade height at the rotor outlet are calculated from

$$A_3 = \frac{\dot{m}}{\rho_3 V_{x3}} \quad (108)$$

$$r_{T3} = \sqrt{\frac{A_3 + \pi r_{H3}^2}{\pi}} \quad (109)$$

$$h_3 = r_{T3} - r_{H3} \quad (110)$$

The stator inlet flow properties can be defined by calculating the stator Mach number  $M_1$  from Eq. (24). Then, using this  $M_1$  value, the static temperature  $T_1$  and pressure  $p_1$  are determined from Eq. (20) and Eq. (23) respectively. The stator inlet density  $\rho_1$  is calculated by using the ideal gas equation, Eq. (18) and the inlet velocity is given by Eq. (19)

$$T_1 = \frac{T_{01}}{1 + \frac{\gamma - 1}{2} M^2} \quad (111)$$

$$p_1 = \frac{p_{01}}{\left(1 + \frac{\gamma - 1}{2} M^2\right)^{\frac{\gamma}{\gamma - 1}}} \quad (112)$$

$$\rho_1 = \frac{p_1}{\mathcal{R}T_1} \quad (113)$$

$$V_1 = M_1 \sqrt{\gamma \mathcal{R}T_1} \quad (114)$$

The blade aspect ratio depends on mechanical and manufacturing considerations [3]. Sieverding [10] states that typical values of the aspect ratio for the stator are ranging from 0.5 to 0.8 and for the rotor from 1.1 to 1.5. From these values we can calculate the chord for both stator and rotor.

The pitch to chord ratio is obtained by applying the Zweifel criterion. In particular, Zweifel's design rule states that losses are minimized for  $0.8 \leq Z \leq 1.0$  [19]. From Eq. (61) and Eq. (62), we can calculate the pitch to chord ratio for both stator and rotor

$$\left(\frac{g}{c}\right)_S = \frac{(p_{01} - P_2)Z}{\rho_2 V_{x2} (V_{\theta 2} - V_{\theta 1})} \quad (115)$$

$$\left(\frac{g}{c}\right)_R = \frac{(p_{02,rel} - P_3)Z}{\rho_2 V_{x2} (w_{\theta 2} - w_{\theta 3})} \quad (116)$$

Knowing the chord, we are able to calculate the pitch for both stator and rotor blades. Finally, we have to chose the stagger angle (Fig. 16).

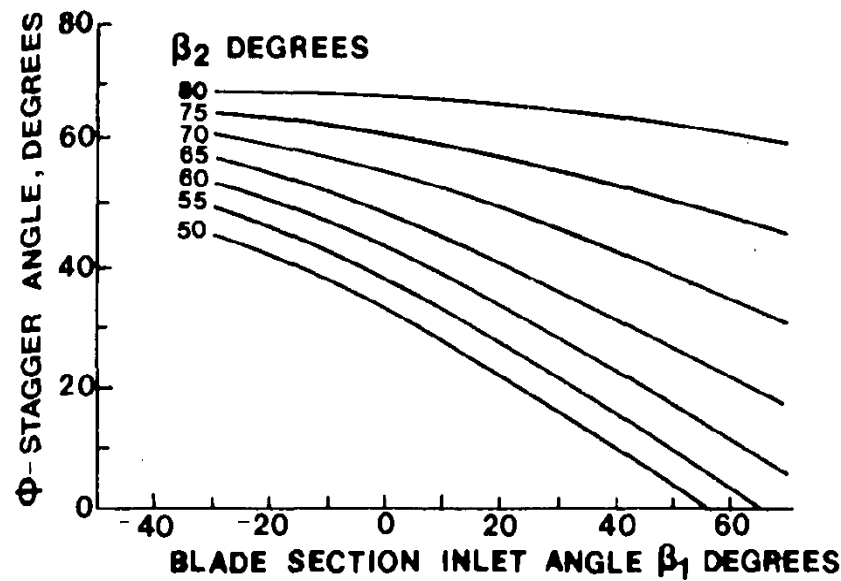


Figure 16. Stagger angle for typical gas turbine blades profiles [21]

Fig. 16 shows typical values of stagger angle based on statistical data. The stagger angle is a function of inlet and outlet angles; absolute flow angles are used for the stator while relative flow angles are used for the rotor [21].

The control of the design can be performed by using the guideline given by [10]:

- 1) For a stage pressure ratio  $\frac{P_3}{P_1}$ , ranging from 3 to 4, in case of high pressure turbines, the stator absolute inlet Mach number should be in the range  $0.85 < M_2 < 1.2$ . If  $M_2 > 1.2$ , we must increase  $R$ . If  $M_2 < 1.2$ , we must decrease  $R$ .
- 2)  $\beta_2$  has a lower limit ranging from  $45^\circ$  to  $50^\circ$  and  $M_{2,rel}$  needs to be lower than 0.5. If these conditions are not respected, there are two actions: we can increase  $\alpha_2$  or we can increase  $R$ .
- 3) For a stage pressure ratio  $\frac{P_3}{P_1}$ , ranging from 3 to 4, in case of high pressure turbines, the stator relative outlet Mach number should be in the range  $0.85 < M_{3,rel} < 1.2$ . If  $M_{3,rel} > 1.2$ , we must decrease  $R$ . If  $M_{3,rel} < 1.2$ , we must increase  $R$ .
- 4) Total turning:  $\Delta\beta \leq 110^\circ \rightarrow 115^\circ$ , if the turning is greater, there are three possible actions: decrease  $\alpha_2$ , decrease  $\beta_3$  or increase  $R$ .

- 5) The blade height ratio should be in the range  $\frac{h_3}{h_2} \leq 1.1 \rightarrow 1.5$ , in case that this condition is not respected, we must decrease  $\beta_3$  or increase  $\alpha_2$ .
- 6) The stator absolute outlet flow angle  $\alpha_3$  should be lower than  $30^\circ$ , if  $\alpha_3 > 30^\circ$  we need to decrease  $\beta_3$ .

Sieverding [10] states that is important to keep a good balance between the stator absolute outlet Mach number  $M_2$  and the rotor relative outlet Mach number  $M_{3,rel}$ .

The mean line design is an iterative method that provides the optimum gas path; this method involves the calculation of velocity triangles, flow properties, and blade row geometries. Using these properties, the design of the turbine airfoil can be started.

## **5 TURBINE AIRFOIL DESIGN**

### **5.1 BLADE PROFILE METHODS**

As stated by Lewis [22], there are two approaches to the blade profile design, the direct and indirect methods.

In the direct method, the designer defines a preliminary blade profile. Then, by means of numerical simulation, the performance parameters are calculated. Analyzing these results and modifying iteratively the geometry, the designer can optimize the blade profile [23].

In the indirect method, conversely, the performance parameters, in terms of pressure and velocity profiles expected, are given; then, the designer, using optimization methods based on numerical simulations and evolutionary algorithms, define the final blade profile [23].

Being this approach more complex and expensive, in this work the direct method will be used. In particular, the first tentative profile will be designed by using the Bézier curve method.

### **5.2 BÉZIER CURVE**

A Bézier curve is a parametric curve that it is used to model smooth profiles. It has been developed by Pierre Bézier while working as engineer for Renault. Bézier curves method has wide applications in the computer aided design, and in the last

years, it has been used as a tool to design turbomachinery airfoils [24]. A Bézier curve of order  $n$  is defined by the following equation:

$$P(t) = \sum_{i=0}^n B_i^n(t) \cdot P_i \quad (117)$$

Where  $P_i$  represent the control points,  $n$  is number of control points – 1,  $t$  is an independent parameter which varies from 0 to 1, and  $B_i^n(t)$  is the Bernstein Polynomial, defined explicitly by

$$B_i^n(t) = \frac{n!}{i!(n-i)!} t^i (1-t)^{n-i} \quad (118)$$

An example of Bézier curves for different values of  $n$  is shown in Fig. 17

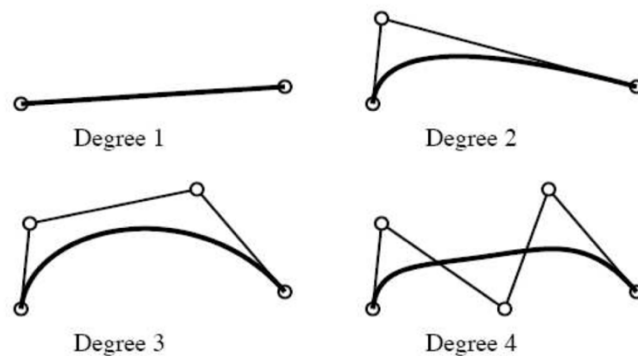


Figure 17. Bézier curves of different degree [25]

From Eq. (118) and Fig. 17, we can see that the Bernstein Polynomial acts as a link between the points on the Bézier curve and the control points; thus for example, 3 control points result in a parabola while 4 control points describe a cubic curve. The parameter  $t$  is used to constrain the first and last control points to lie on the Bézier curve, while the other control points define the shape of the curve.

The first derivate of a Bézier curve of  $n$  degree is



$$\frac{dP(t)}{dt} = n \sum_{i=0}^{n-1} (P_{i+1} - P_i) B_i^{n-1}(t) \quad (119)$$

This equation is useful to calculate the slope of the line tangent to these curves at a given point.

### 5.3 DESIGN APPROACH

Pritchard [26] states that there are at least 25 airfoils parameters that can be associated with any blade shape. A turbine designer must sort out which of these parameters are known with absolute certainty. From Chapter 4, we are able to specify the inlet and outlet flow angles, the pitch, the chord, and the stagger angle. The leading edge radius  $r_{LE}$  and trailing edge radius  $r_{TE}$  are limited by mechanical constraints such as maximum stress and deformation. Being these 7 parameters fixed, the turbine designer can use only the curvature as a free parameter, that is the control points of the Bézier curve. A MATLAB code has been written to design the turbine airfoil.

Based on the techniques developed by Verstraete [27], and Sousa and Paniagua [28], the turbine blade profile design starts by the definition of a camberline, as shown in Fig. 18, which depends on the inlet blade metal angle  $\beta_{in}$ , the outlet blade metal angle  $\beta_{out}$ , the chord  $c$ , and the stagger angle  $\Phi$ .

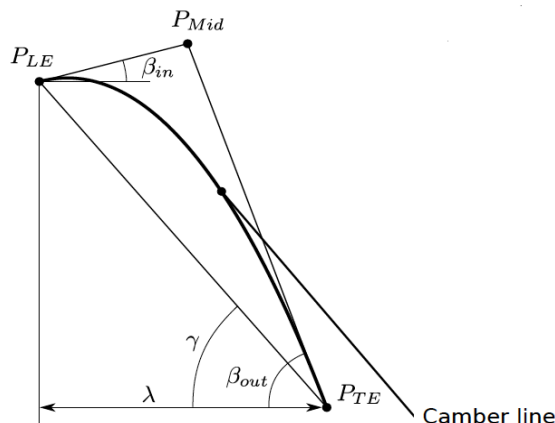


Figure 18. Camber line construction [27]

The leading edge point  $P_{LE}$ , the middle point  $P_{Mid}$ , and the trailing edge point  $P_{TE}$  are the control points of the Bézier curve that describe the camber line. The  $P_{LE}$  point is the origin of the coordinate system. The  $P_{TE}$  point is defined by the axial chord  $c_x$  and the stagger angle  $\Phi$ . The  $P_{Mid}$  is the intersection between the line starting from the point  $P_{LE}$  and the line coming from  $P_{TE}$ . Then, we have:

$$P_{LE} = (0,0) \quad (120)$$

$$P_{TE} = (c \cos \Phi, c \cos \Phi \tan \Phi) \quad (121)$$

$$P_{Mid,x} = \frac{P_{LE,y} - P_{LE,x} \tan \beta_{in} - P_{TE,y} + P_{TE,x} \tan \beta_{out}}{\tan \beta_{out} - \tan \beta_{in}} \quad (122)$$

$$P_{Mid,y} = P_{LE,y} + \tan \beta_{in} (P_{Mid,x} - P_{LE,x}) \quad (123)$$

To construct the camber line, we have 3 control points, thus a polynomial of second order. From Bézier curve equations, Eq. (117) and Eq. (118), we can obtain the  $x$  and  $y$  coordinates of the camber line

$$P_{camber,x} = (1 - t)^2 P_{LE,x} + 2(1 - t) P_{Mid,x} + t^2 P_{TE,x} \quad (124)$$

$$P_{camber,y} = (1 - t)^2 P_{LE,y} + 2(1 - t) P_{Mid,y} + t^2 P_{TE,y} \quad (125)$$

The suction and pressure sides are also defined by the Bézier curves, whose control points are specified by the normal distance relative to the camber line. The first and last control points are the leading and trailing edge points respectively. For the second control point of both sides the distance is computed by using the leading edge radius; in this way, we can guarantee the minimum thickness of the leading edge. The second last control point for both sides is specified by the trailing edge radius. The

reason to use this point is to guarantee the minimum thickness of the trailing edge. In order to keep the geometric continuity of the trailing edge region, we need a third last control point for both sides, which depends on the trailing edge wedge angle  $\alpha_{LE}$ . In this work, the suction side is defined by using 10 control points, 5 of them being free parameters while the pressure side is defined by 8 control points, 3 of them being also free design parameters. The reason of using more control points for the suction side with respect to those used for the pressure side, is that the losses production is higher on suction side; therefore, the turbine designer needs to have finer control of the curvature on the suction side.

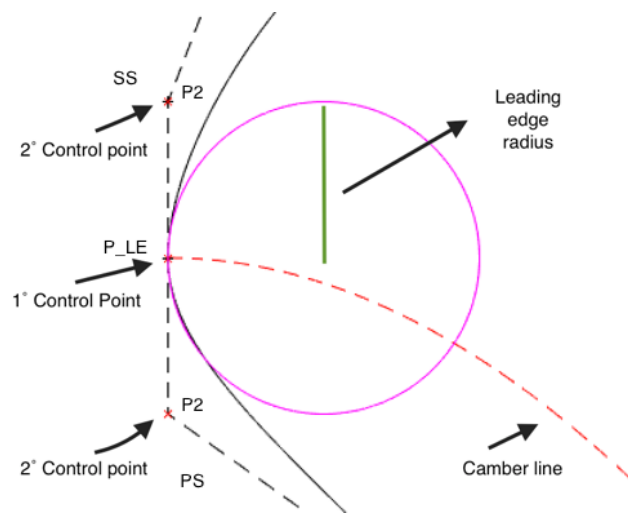


Figure 19. Leading edge parameterization

The positions of the second control point of the suction and pressure side are defined by:

$$P_{2x,SS} = P_{LE,x} - r_{LE} \cos(90 - \beta_{in}) \quad (126)$$

$$P_{2y,SS} = P_{LE,y} + r_{LE} \sin(90 - \beta_{in}) \quad (127)$$

$$P_{2x,PS} = P_{1x,SS} + r_{LE} \cos(90 - \beta_{in}) \quad (128)$$

$$P_{2y,PS} = P_{1y,SS} - r_{LE} \sin(90 - \beta_{in}) \quad (129)$$

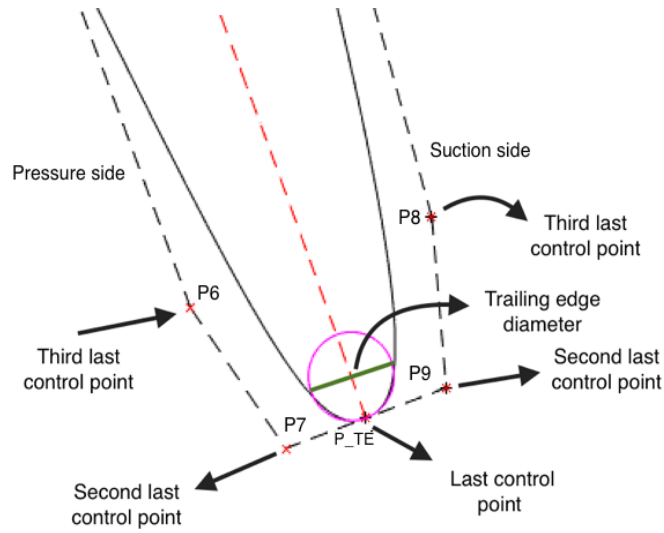


Figure 20. Trailing edge parameterization

The positions of the second last control point of the suction and pressure side are

$$P_{9x,SS} = P_{TE,x} + 2r_{TE} \cos(\beta_{out} + 90) \quad (130)$$

$$P_{9y,SS} = P_{TE,y} + 2r_{TE} \sin(\beta_{out} + 90) \quad (131)$$

$$P_{7x,PS} = P_{TE,x} - 2r_{TE} \cos(\beta_{out} + 90) \quad (132)$$

$$P_{7y,PS} = P_{TE,y} - 2r_{TE} \sin(\beta_{out} + 90) \quad (133)$$

The positions of the third last control point of the suction and pressure side are

$$P_{8x,SS} = P_{9x,SS} - \frac{r_{TE}}{2 \sin \alpha_{LE}} \cos(\alpha_{LE} - \beta_{out}) \quad (134)$$

$$P_{8y,SS} = P_{9y,SS} + \frac{r_{TE}}{2 \sin \alpha_{LE}} \sin(\alpha_{LE} - \beta_{out}) \quad (135)$$

$$P_{6x,PS} = P_{7x,PS} - \frac{r_{TE}}{2 \sin \alpha_{LE}} \cos(-\alpha_{LE} - \beta_{out}) \quad (136)$$

$$P_{6y,PS} = P_{7y,PS} + \frac{r_{TE}}{2 \sin \alpha_{LE}} \sin(-\alpha_{LE} - \beta_{out}) \quad (137)$$

The suction side parameterization is shown in Fig. 21. The point  $i$  on the camber line  $(X_i, Y_i)$  and the distance  $d_i$  from this point to the control point  $P_{i,SS}$  are free choices of the designer. In order to draw the suction side curve, it is necessary to find the position of the control points ( $P_3$  to  $P_7$ ). The coordinates of these control points are calculate by

$$P_{ix,SS} = X_{i,camber} + d_i \cos(\varphi_{i,SS}) \quad (138)$$

$$P_{iy,SS} = Y_{i,camber} + d_i \sin(\varphi_{i,SS}) \quad (139)$$

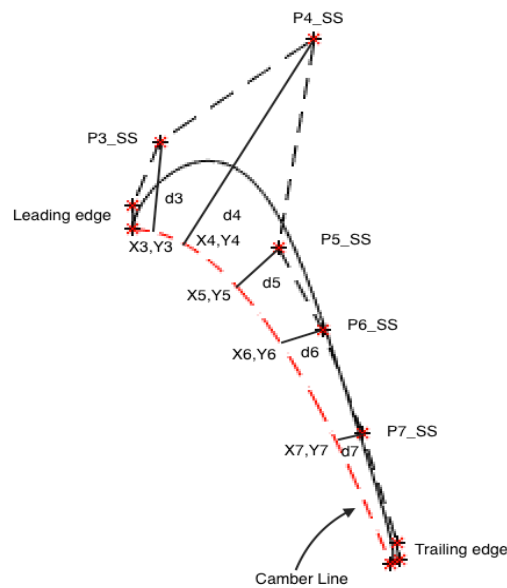


Figure 21. Suction side parameterization

Where  $\varphi_i$  is the slope angle of the line normal to the camber line curve at the point  $(X_i, Y_i)$

$$\tan \varphi_{i,SS} = -\frac{1}{\tan a_i} \quad (140)$$

In order to calculate  $\varphi_{i,SS}$ , we have to define the slope of the tangent line to the camber line curve at  $(X_i, Y_i)$ . By definition, the slope of the tangent line,  $\tan a$ , is defined by:

$$\tan a_i = \frac{dP_{iy,camber}}{dP_{ix,camber}} \quad (141)$$

The derivatives above are calculated by Eq. (119) or by doing the derivative of equations, Eq. (124) and Eq. (125).

The control points of the pressure side are obtained in a similar way, Fig. 22. The difference is in the number of control points ( $P_3$  to  $P_5$ ), thus in the position of the camber line points, and in the slope of the normal line, which is defined by

$$\varphi_{i,PS} = 90 - a_i \quad (142)$$

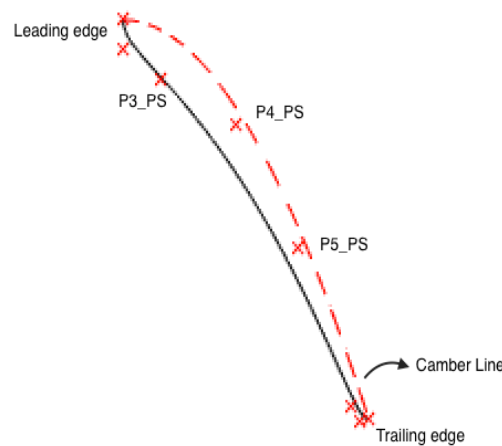


Figure 22. Pressure side parameterization

With the control points of both sides defined, from Bézier curve equations, Eq. (117) and Eq. (118), we can obtain the suction and pressure side curves, thus the turbine airfoil.

- Suction side

$$\begin{aligned}
 x_{SS} = & (1-t)^9 P_{LE,x} + 9t(1-t)^8 P_{2x,SS} + 36t^2(1-t)^7 P_{3x,SS} \\
 & + 84t^3(1-t)^6 P_{4x,SS} + 126t^4(1-t)^5 P_{5x,SS} \\
 & + 126t^5(1-t)^4 P_{6x,SS} + 84t^6(1-t)^3 P_{7x,SS} \\
 & + 36t^7(1-t)^2 P_{8x,SS} + 9t^8(1-t) P_{9x,SS} \\
 & + t^9 P_{TE,x}
 \end{aligned} \tag{143}$$

$$\begin{aligned}
 y_{SS} = & (1-t)^9 P_{LE,y} + 9t(1-t)^8 P_{2y,SS} + 36t^2(1-t)^7 P_{3y,SS} \\
 & + 84t^3(1-t)^6 P_{4y,SS} + 126t^4(1-t)^5 P_{5y,SS} \\
 & + 126t^5(1-t)^4 P_{6y,SS} + 84t^6(1-t)^3 P_{7y,SS} \\
 & + 36t^7(1-t)^2 P_{8y,SS} + 9t^8(1-t) P_{9y,SS} \\
 & + t^9 P_{TE,y}
 \end{aligned} \tag{144}$$

- Pressure side

$$\begin{aligned}
 x_{PS} = & (1-t)^7 P_{LE,x} + 7t(1-t)^6 P_{2x,PS} + 21t^2(1-t)^5 P_{3x,PS} \\
 & + 35t^3(1-t)^4 P_{4x,PS} + 35t^4(1-t)^3 P_{5x,PS} \\
 & + 21t^5(1-t)^2 P_{6x,PS} + 7t^6(1-t) P_{7x,PS} \\
 & + t^7 P_{TE,x}
 \end{aligned} \tag{145}$$

$$\begin{aligned}
 y_{PS} = & (1-t)^7 P_{LE,y} + 7t(1-t)^6 P_{2y,PS} + 21t^2(1-t)^5 P_{3y,PS} \\
 & + 35t^3(1-t)^4 P_{4y,PS} + 35t^4(1-t)^3 P_{5y,PS} \\
 & + 21t^5(1-t)^2 P_{6y,PS} + 7t^6(1-t) P_{7y,PS} \\
 & + t^7 P_{TE,y}
 \end{aligned} \tag{146}$$

Fig. 23 shows an example of turbine airfoil generated by the MATLAB code, which is based on the procedure discussed.

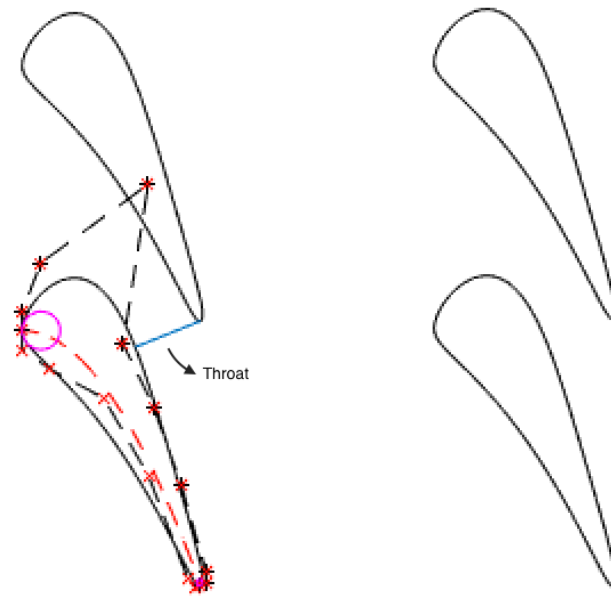


Figure 23. Axial turbine airfoil

Noticed that the throat region can be controlled by adjusting the control points of both surfaces in order to obtain the required throat size.



## REFERENCES

- [1] Denton, J.D. Loss mechanisms in turbomachines. *J. Turbomach.* 1993, 115, 621-656.
- [2] General Electric. Retrieved June 19, 2016, from <http://www.ge.com/digital/>
- [3] Mattingly, J., *Elements of Propulsion: Gas Turbine and Rockets*, AIAA Education Series., 2006.
- [4] Anderson J.D., *Computational Fluid Dynamics, the Basics with applications*, McGraw-Hill, 1995.
- [5] Tomita, J.T., “Three-Dimensional Flow Calculations of Axial Compressor and Turbines Using CFD Techniques”, PhD thesis, Technical Institute of Aeronautics, São José dos Campos, Brazil, 2008.
- [6] Ainley, D. G. and Mathieson, G. C. R., 1951, “A method of performance estimation for axial flow turbines”. ARC R. and M. 2974.
- [7] Dixon, S. L., Hall, C. A., *Fluid Mechanics and Thermodynamics of Turbomachinery*, 7<sup>th</sup> Ed, Butterworth-Heinemann, 2014.
- [8] Anderson, J. D., *Modern compressible flow*, McGrawHill, 2004.
- [9] Çengel, Y. A and Boles M. A, *Thermodynamics: An Engineering Approach*, 5<sup>th</sup> Ed, McGraw-Hill, 2006.
- [10] Lakshminarayana, B., *Fluid dynamics and heat transfer of turbomachinery*, John Wiley & Sons, 1996.
- [11] White F. M., *Fluid mechanics*, 7<sup>th</sup> ed, McGrawHill, 2011.
- [12] Turns S. R., *An introduction to combustion: concepts and applications*, 3<sup>th</sup> Ed, McGrawHill, 2012.
- [13] Traupel W., *Thermische Turbomaschinen*, Vol 1, 3<sup>rd</sup> Ed, Springer, 1977.
- [14] Sieverding C. R., 2012. Unpublished note. Advanced Course on Turbines. Von Karman Institute for Fluid Dynamics.
- [15] Wilson D.G. *The Design of High-efficiency Turbomachinery and Gas Turbines*. The MIT Press, 1984.
- [16] Kenny S., “Development of a multi-disciplinary design tool for axial flow turbines,” Master’s thesis, Carleton University, Ottawa, Canada, 2005.

- [17] Dahlquist, A. D. "Investigation of losses prediction methods in 1D axial gas turbines," Master's thesis, Lund University, Lund, Sweden, 2008.
- [18] Xu, L., and Denton, J. D., 1988, "The Base Pressure and Loss of a Family of Four Turbine Blades," ASME JOURNAL OF TURBOMACHINERY, Vol. 110, pp. 9-17.
- [19] Zweifel, O. 1945, "The spacing of turbomachine blading, especially with large angular deflection," Brown Boveri Review, 32.12.
- [20] Taylor, M., "HP Axial Flow Turbine Aerodynamic Design," Advances in Turbomachinery Aero-Thermo-Mechanical Design and Analysis, VKI Lecture Series, von Karman Inst. for Fluid Dynamics, Rhode-Saint-Genèse, Belgium, Nov. 2006.
- [21] Kacker, S.C., Okapuu U., 1982, "A mean line prediction method for axial flow turbine efficiency," Journal of Engineering Power. Transaction of the American Society of Mechanical Engineers, 104, 111-119.
- [22] Lewis, R. I., Turbomachinery performance analysis, Elsevier Science & Technology Books, 1996.
- [23] Korakianitis T., Rezaenia M.A., Hamakhan I.A., Wheeler A.P.S. (2013). Two- and three-dimensional prescribed surface curvature distribution blade design (circle) method for the design of high efficiency turbines, compressors, and isolated airfoils. *Journal of Turbomachinery*, 135 (3), art. no. 041002.
- [24] Farin, G., Curves and Surfaces For Computer Aided Geometric Design, 4<sup>th</sup> Ed, Academic Press, 1997.
- [25] Sederberg, T. W., 2012. Computer Aided Geometric Design Course Notes. Brigham Young University.
- [26] Pritchard, L. J. An eleven parameter axial turbine airfoil geometry model. ASME 85-GT-219; 1985.
- [27] Verstraete, T.: CADO: a computer aided design and optimization tool for turbomachinery applications EngOpt2010, 2<sup>nd</sup> International Conference on Engineering Optimization, Lisbon, Portugal, September 6-9, 2010.
- [28] Sousa, J.; Paniagua, G. Entropy Minimization Design Approach of Supersonic Internal Passages. *Entropy* 2015, 17, 5593-5610.